For numerical calculation of B_g, we rewrite (22) as

$$B_g = \frac{2}{\pi} \frac{kb}{\sqrt{\frac{\mu}{\epsilon}}} S(\Delta, c) \tag{24}$$

where

$$\Delta = d/(b-a), \qquad c = b/a \tag{25a}$$

and

$$S(\Delta, c) = \sum_{n=1}^{\infty} \frac{(1-e^{-2n\pi\Delta})(c-1)[J_1(\gamma_n b)N_0(\gamma_n a) - J_0(\gamma_n a)N_1(\gamma_n b)]}{n^2\Delta(c[J_1(\gamma_n b)N_0(\gamma_n a) - J_0(\gamma_n a)N_1(\gamma_n b)] - [J_1(\gamma_n a)N_0(\gamma_n b) - J_0(\gamma_n b)N_1(\gamma_n a)])}. \tag{25b}$$

The approximate values (16) and (14) are used.

Fig. 5 shows the results of a digital computer evaluation of $S(\Delta, c)$ for $c = 5$. If $c = b/a \to 1$ (with Δ kept finite), then $S(\Delta, c)$ tends to

$$S(\Delta, 1) = \sum_{n=1}^{\infty} \frac{1-e^{-2n\pi\Delta}}{n^2\Delta} = \frac{1}{\Delta}\left[\frac{\pi^2}{6} - \sum_{n=1}^{\infty} \frac{e^{-2n\pi\Delta}}{n^2}\right]. \tag{26}$$

An approximate evaluation of this series can be made, for various Δ, on a programmable pocket calculator. $S(\Delta, 1)$ has been plotted on Fig. 5. Notice how close in value are the curves $S(\Delta, 1)$ and $S(\Delta, 5)$. Other curves for $S(\Delta, c)$, where $1 < c < 5$, lie in the narrow band between the two curves shown in Fig. 5. Because of the insensitivity of $S(\Delta, c)$ to variations in b/a, it is a reasonable approximation to use $S(\Delta, 1)$ for $S(\Delta, c)$ whenever $1 < b/a \leqslant 5$.

For $\Delta \leqslant 0.01$, there is a useful asymptotic expression for (26):

$$S(\Delta, 1) \sim 2\pi \ln\left(\frac{e}{2\pi\Delta}\right). \tag{27}$$

The error obtained in using (27) to approximate (25b) is about 1.7 percent when $\Delta = 0.01$, $b/a = 5$, and shrinks with shrinking Δ or b/a.

III. Numerical Example

A lossless line has $b = 1$ cm and $b/a = 3$. For the material between the conductors, $\mu = \mu_0$ and $\epsilon = 2.24\ \epsilon_0$. The characteristic impedance is $Z_0 = 44.0\ \Omega$. Let a load of $Z_A = 44\ \Omega$ be placed in a gap of width d described by $\Delta = d/(b-a) = 0.1$. A computer evaluation of (25b) gives $S(0.1, 3) = 10.29$ (note that (26) would yield 9.20). If $f = 600$ MHz, we have, from (24), $B_g = 4.89 \times 10^{-3}\ \mho$. This capacitive susceptance in parallel with Z_A yields an effective load impedance of $42.05 - j\ 9.05\ \Omega$, which is moderately different from Z_A.

In this example, the width of the gap is 0.067 cm, which is 2/1000 of the wavelength λ in the line. One should not use the procedure described here unless the gap is very narrow compared to λ, as the theory fails to account for any distribution of the load along the line but assumes it to be concentrated at one location.

Acknowledgment

The author gratefully acknowledges help from Prof. R. W. P. King of Harvard University, who interested him in this problem, and from Prof. Hao Ming Shen of the Chinese Academy of Sciences, who assisted him in obtaining the result in (27).

References

[1] D. A. Hill and J. R. Wait, "Electromagnetic fields of a coaxial cable with an interrupted shield located in a circular tunnel," *J. Appl. Phys.*, vol. 46, no 10, pp 4352–4356, Oct. 1975

[2] D. A. Hill and J. R. Wait, "Scattering from a break in the shield of a braided coaxial cable—Numerical results," *Arch. Elek. Übertragung.*, vol. 30, no. 3, pp 117–121, Mar. 1976.

[3] S. A. Schelkunoff, *Electromagnetic Waves*. New York, Van Nostrand, 1943, pp. 418–421.

[4] H. Dwight, "Natural frequencies in coaxial type cavities," *J. Math. Phys.*, vol. 27, no. 1, pp. 84–89, 1948.

Depth of Penetration of Fields from Rectangular Apertures into Lossy Media

ERIK CHEEVER, JONATHAN B. LEONARD, AND KENNETH R. FOSTER, SENIOR MEMBER, IEEE

***Abstract*—A widely used device for biomedical applications of microwave energy is the dielectric-loaded waveguide operating in the TE_{10} mode. We have calculated the $(1/e)$ energy penetration depth from such antennas, modeled as rectangular apertures radiating into a lossy medium with dielectric properties resembling those of tissue. The results are presented in nondimensional form from which the characteristics of practical antennas can be estimated. Depending on the dielectric properties of the medium and the size of the aperture, the effective penetration depth can be limited by either the aperture size or the plane-wave penetration depth; practical antennas fall between these two extremes. Experimental results confirm the calculations.**

I. Introduction

Several medical applications of microwave energy have been developed that heat tissue (diathermy and hyperthermia) or measure tissue temperature from the microwave energy that is passively emitted from the body (radiometry). The simplest antenna for such purposes (and one that is widely used) is a rectangular waveguide placed against the surface of the body [1]–[3].

An important consideration is the effective depth of heating or sensing. The field patterns in the tissue beneath an aperture can be calculated using well-established theory [4], [5]. However, these calculations are complex, and in discussing such applications investigators frequently cite the plane-wave penetration depth in the tissues. In contrast, the heating or sensing occurs primarily in the near field of the antenna with a sensitivity function that depends strongly on both the antenna geometry and the material properties of the medium. It is apparent that the effective depth of heating or sensing can be far less than the energy penetration depth of plane waves. We report the penetration depth of energy from rectangular apertures in nondimensionalized form that can be easily applied to a variety of situations. This is a generalization of results previously reported by Turner [6].

Manuscript received November 28, 1986; revised April 20, 1987.

The authors are with the Department of Bioengineering, University of Pennsylvania, Philadelphia, PA 19104

IEEE Log Number 8715663

II. Methods

Following the development in Stratton [7], the wave equation can be cast in dimensionless form by normalizing distance to a characteristic length a. The natural choice for this parameter is the aperture width, which determines the cutoff frequency of the principal mode (TE_{10}) of the guide. The dimensionless wave number K for radiation in tissue is then defined as

$$K = ka = \omega(\epsilon_0 \mu_0 \epsilon^*)^{1/2} a \tag{1}$$

where $\omega/2\pi$ is the frequency in Hz, μ_0 and ϵ_0 are the free-space permeability and permittivity, and ϵ^* is the complex relative permittivity of the medium. The dimensionless parameter K contains the significant parameters for the design of the antenna: the frequency, the dielectric properties of the tissue, and the antenna size; the normalized penetration depth is calculated as a function of this parameter. For the calculations presented below, a 2:1 aspect ratio was assumed for the aperture, corresponding to a normalized aperture width of 1 and a height of 1/2. In all cases single-mode operation was assumed, with the guide operating at a frequency midway between cutoff for TE_{10} and TE_{20} modes.

Most of the calculations employed the mode-matching technique as described by Harrington [8]. The rectangular aperture is modeled as a rectangular waveguide opening into a much larger waveguide filled with the tissue dielectric. The field distribution in the larger guide is calculated as a superposition of its normal modes:

$$Ey(Z) = \sum_{\substack{m=1 \\ \text{odd}}}^{\infty} \sum_{n=0}^{\infty} E_{mn} \cos\left(\frac{m\pi X}{C}\right) \cos\left(\frac{n\pi Y}{D}\right) e^{-\gamma_{mn} Z} \tag{2}$$

where

$$\gamma_{mn} = \sqrt{\left(\frac{m\pi}{C}\right)^2 + \left(\frac{n\pi}{D}\right)^2 - K^2}$$

and C and D are the dimensions of the larger guide, normalized to the width of the aperture, a. The origin of the coordinate system is taken as the center of the aperture, with the Z axis projecting into the medium normal to the plane of the aperture. Only those values of m and n for which the fields satisfy the required boundary conditions at the walls of the guide are allowed. The field in the aperture was assumed to correspond to the TE_{10} mode for the smaller guide:

$$Ey = \begin{cases} E_0 \cos(\pi X) & |Y| \leq \frac{1}{4}, |X| \leq \frac{1}{2} \\ 0 & \text{otherwise} \end{cases} \tag{3}$$

where the aperture width and height are 1 and 1/2, respectively, in normalized units. The coefficients E_{mn} are then obtained from the requirement

$$E_{mn} = (8\epsilon_n / CD) \int_0^{1/4} \int_0^{1/2} \cos(\pi X) \cos(m\pi X/C) \cdot \cos(n\pi Y/D)\, dY\, dX \tag{4}$$

where

$$\epsilon_n = \begin{cases} 1 & n = 0 \\ 2 & n = 1, 2, \cdots. \end{cases}$$

This model is an approximation in several respects. First, (2)–(4) provide a discrete approximation to the fields because of the finite dimensions of the larger guide. Second, the model assumes that the plane that separates the two guides is a perfect conductor except at the opening of the smaller guide. Finally, the model assumes that the field distribution over the aperture corresponds to the TE_{10} mode of the smaller guide; in reality the aperture field corresponds to a superposition of incident and reflected TE_{10} and evanescent higher modes propagating back into the smaller guide. However, repeated calculations in which the dimensions of the larger guide were varied show that errors of the first kind are negligible. (For most of the calculations reported below $C = 8$ and $D = 4$.) Experimental data, discussed below, show that these approximations are adequate for present purposes. Important advantages of the mode-matching technique are its ease and speed of calculation.

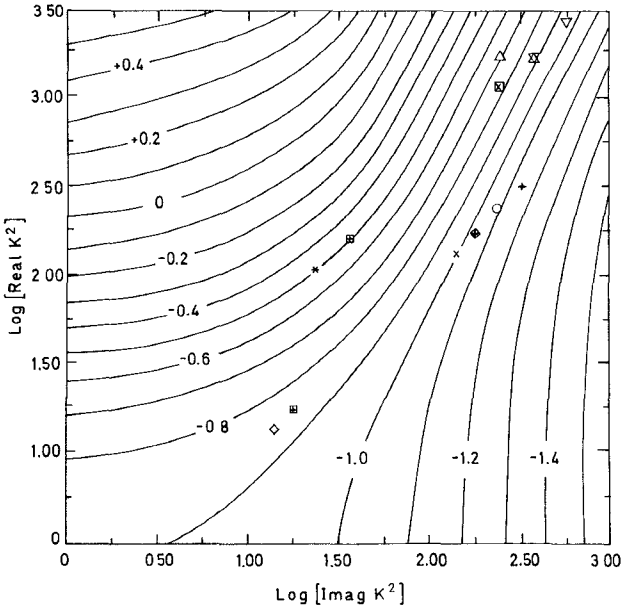

Fig. 1. Contour plot showing the penetration depth of the energy beneath the rectangular aperture, normalized by a, the width of the aperture. The abscissa and ordinate represent the real and imaginary parts of the square of the complex wavenumber for the radiation in the medium, normalized by the aperture width (eq. (1)). The symbols indicate the squares of the complex wavenumbers for the apertures and liquids summarized in Table I. All values are given as common logarithms.

The fields were calculated along the Z axis, i.e., along the perpendicular line extending from the center of the aperture into the medium. The energy penetration depth was taken to be the position on the line at which the power density was reduced by a factor $1/e$ from that at the aperture plane. More than 200 calculations were done for different values of the nondimensionalized parameters, and the results interpolated to produce the contour plots shown in Fig. 1.

Several tests were performed to ensure the accuracy of the results. For all of the cases in which experimental data were obtained, the mode-matching calculations were checked using the plane-wave spectrum method [8]. In addition, selected results were confirmed by direct integration of the vector potential equations [8]. All of these results were in excellent agreement.

As a final test of the calculations, the energy penetration depth was measured using three different apertures and two liquids (water and ethanol). A small sensing antenna was mounted on a movable jig, and the transmission coefficient between the waveguide and the antenna was measured using a network analyzer (Hewlett-Packard model 8410). Since the ethanol contained a small fraction of water, its dielectric properties were measured using techniques previously described [9]. The measured penetration depths agreed well with the calculations (Table I) within an experimental uncertainty of roughly 0.1 cm.

TABLE I
CALCULATED AND MEASURED ENERGY PENETRATION DEPTHS FOR APERTURES RADIATING INTO WATER OR ETHANOL COMPARED WITH THE PLANE-WAVE PENETRATION DEPTH

Aperture Width (cm)	Symbol	Frequency (GHz)	Liquid	Permittivity		Penetration Depth (cm)		
				ϵ'	ϵ''	Calculated	Measured	Plane Wave
7.3	○	3.1	ethanol	10.8	10.5	.56	.6	.53
7.3	+	3.9	"	9.1	9.3	.46	.4	.44
4.8	×	3.9	"	9.1	9.3	.46	.4	.44
4.8	⊕	4.7	"	8.0	8.2	.41	.4	.39
1.5	◇	3.9	"	9.1	9.3	.20	.2	.44
1.5	⊞	4.7	"	8.0	8.2	.21	.2	.39
7.3	△	3.1	water	77.0	11.0	1.01	1.2	1.23
7.3	▽	3.9	"	75.0	16.0	.67	.7	.67
4.8	⊠	3.9	"	75.0	16.0	.64	.6	.67
4.8	⧆	4.7	"	74.0	17.0	.49	.5	.52
1.5	*	3.9	"	75.0	16.0	.49	.5	.67
1.5	⊞	4.7	"	74.0	17.0	.47	.4	.52

The dielectric properties of the ethanol are measured values, which differ slightly from literature values because of slight contamination by water.

The symbols indicate the locations of these apertures on Fig. 1.

III. Results and Discussion

Fig. 1 shows the logarithm of the normalized penetration depth δ as a function of the square of the wavenumber K defined in (1). The range of the abscissa corresponds to aperture widths roughly 0.5 to 8 times the wavelength of the radiation in the medium for reasonable values of the parameters. This method is presentation allows easy calculation of the effective penetration depth: the aperture width and the complex permittivity of the medium determine the real and imaginary parts of K^2 and thus the coordinates on the figure. The contour at that location then gives the logarithm of the normalized penetration depth.

Two distinct regions appear in the figure, representing different limiting cases: the upper left part and the right part.

In the upper left part of the figure, the penetration depth is essentially independent of the abscissa. A numerical correlation shows that with $\epsilon''/\epsilon' < 0.25$ and $\log(\omega^2\mu_0\epsilon_0\epsilon' a^2) > 1$, the effective penetration depth δ is given approximately by

$$\delta = d/a \simeq 0.4\left[a\sqrt{\epsilon'}/\lambda^*\right]^{1.4} \tag{5}$$

where λ^* is the wavelength of the radiation in the medium and d is the effective penetration depth in dimensional units. In this region the aperture is electrically small and its size determines the penetration depth.

In the right part of the figure, the penetration depth is independent of the ordinate and approaches the plane-wave energy penetration depth:

$$d = \frac{\lambda_0}{2\pi\sqrt{2\epsilon'}}\left[\left(1+(\epsilon''/\epsilon')^2\right)^{1/2}-1\right]^{-1/2} \tag{6}$$

where λ_0 is the free-space wavelength.

These limits represent upper and lower bounds of the effective penetration depth of the energy in the medium. Practical apertures might approach either limit in biomedical applications. In particular, in the frequency range 0.1–1 GHz, apertures used for local hyperthermia treatments are electrically small and their depths of effective heating would most likely be determined by their dimensions rather than by the plane-wave penetration depth of the energy in the tissue. The present results provide a simple way to estimate this important quantity.

Acknowledgment

The authors thank M/A-COM, Inc. for the loan of equipment, in particular K. L. Carr for his interest and encouragement in this study. They also thank Dr. C. Grosse for helpful comments on an earlier version of this manuscript.

References

[1] J. W. Hand and A. J. Hind, "A review of microwave and RF applicators for localized hyperthermia," in *Physical Techniques in Clinical Hyperthermia*, J. W. Hand and J R. James, Eds. New York: Wiley, 1986, pp. 98–147.
[2] J. Bach Anderson, "Theoretical limitations on radiation into muscle tissue," *Int. J Hyperthermia*, vol. 1, pp. 45–55, 1985.
[3] J. Schaeffer, A. M. El-Mahdi, and K. L. Carr, "Thermographic detection of human cancers by microwave radiometry," in *Biomedical Thermology*, G. Nussbaum, Ed. New York: Alan R. Liss, 1982, pp. 509–521.
[4] S. S. Stuchly and M. A. Stuchly, "Multimode square waveguide applicators for medical applications of microwave power," in *Proc. 8th European Microwave Conf.*, 1978, pp. 553–557.
[5] A W. Guy, "Electromagnetic fields and relative heating pattern due to a rectangular aperture source in direct contact with bilayered biological tissue," *IEEE Trans. Microwave Theory Tech.*, vol. MTT-19, pp. 214–223, 1971.
[6] P. F. Turner, "Computer solution for applicator heating patterns," in *National Cancer Institute Monograph 61*, L. A. Dethlefsen, Ed. NIH Publication 82-2437, Bethesda MD, 1982.
[7] J. A. Stratton, *Electromagnetic Theory*. New York: McGraw-Hill, 1941.
[8] R. F. Harrington, *Time Harmonic Electromagnetic Fields*. New York: McGraw-Hill, 1961.
[9] J L. Schepps and K. R. Foster, "UHF and microwave dielectric properties of normal and tumor tissues: Variation in dielectric properties with tissue water content," *Phys. Med. Biol.*, vol. 25, pp 1149–1159, 1980.